

- tion,” *IEEE Trans. Pattern Analysis and Machine Intelligence*, PAMI-5,4, July 1983.
- [15] Bolles, R.C. and Horaud, P., “3DPO: A three-dimensional part orientation system,” in *Three-Dimensional Machine Vision*, Kluwer, Boston, MA, 1987.
- [16] Koenderink, J.J. and Van Doorn, A.J., “The Singularities of the Visual Mapping,” *Biological Cybernetics*, 24(1), 1976
- [17] Chin, R.T. and Dyer, C.R. “Model-based recognition in robot vision” , *ACM Computing Surveys*, 18(1), 1986.

Reference

- [1] Gauss, K. F., *General Investigations of Curved Surfaces*, Raven Press, New York, 1965.
- [2] Lysternik, L.A., *Convex Figures and Polyhedra*, Dover Publications, New York, 1963.
- [3] Horn, B.K.P., "Extended Gaussian Image," *Proc. of IEEE*, Vol. 72, No. 12, pp.1671-1686, December 1984.
- [4] Ikeuchi, K., "Recognition of 3-D Objects using the Extended Gaussian Image," *Proc. of Intern. Joint Conf on Artificial Intelligence*, Vancouver, B.C., pp.595-600, August 1981.
- [5] Brou, P., "Using the Gaussian Image to Find the Orientation of Objects," *Intern. Journal of Robotics Research*, Vol. 3, No. 4, pp. 89-125, Winter 1984.
- [6] Little, J. J., "Determining Object Attitude from Extended Gaussian Image," *Proc. of Intern. Joint Conf on Artificial Intelligence*, Los Angeles, California, pp. 960-963, August 1985.
- [7] Ikeuchi, K. and Horn, B.K.P., "Picking up an Object from a Pile of Objects," in *Robotics Research: The First International Symposium*, J. M. Brady & R. Paul (eds.), MIT Press, Cambridge, Massachusetts, pp. 139-162, 1984.
- [8] Kang, S.B. and Ikeuchi, K., "The Complex EGI: New Representation for 3-D Pose Determination," *IEEE Trans Pattern Analysis and Machine Intelligence*, Vol. 15, No. 7, pp. 707-721, July 1993.
- [9] Nalwa, V. S., "Representing Oriented Piecewise C2 Surfaces," *Proc. 2nd Intern. Conf. on Computer Vision*, pp. 40-51, December 1988.
- [10] Roach, J. W. Wright, J.S., and Ramesh, V., "Spherical Dual Images: A 3-D Representation Method for Solid Objects that Combines Dual Space and Gaussian Sphere," *Proc. IEEE Conf on Computer Vision and Pattern Recognition*, pp. 236-241, June 1986.
- [11] Dellinette, H., Hebert, M., and Ikeuchi, K., "A Spherical Representation for the Recognition of Curved Objects," *Proc. Intern. Conf on Computer Vision*, pp.103-112, May 1993.
- [12] Besl, P. and Kay, N.D., "A Method for Registration of 3-D Shapes," *IEEE Trans Patern Analysis Machine Intelligence*, Vol. 14, No.2, Feb 1992.
- [13] Higuchi, K. Delinette, H. Hebert, M. and Ikeuchi, K., "Merging Multiple Views using a Spherical Representation," *Proc. IEEE Workshop on CAD-based Vision*, pp.124-131, Feb 1993.
- [14] Oshima, M. and Shirai, Y., "Object recognition using three-dimensional informa-

Acknowledgments

The research described in this paper was done with our former and current students, Dr. Sing Bing Kang of DEC Cambridge Research Lab, Dr. Herve Delingette of INRIA Sophia-Antipolis, Dr. Kazunori Higuchi of Toyota Central Research Lab, and Harry Shum of CMU.. Their contributions are greatly appreciated.

4. Conclusion

In this paper, we argued that main issue in representing general objects is to be able to define an intrinsic coordinate system on a surface, onto which properties such as curvature may be mapped. A convenient way of addressing this problem is to define an intrinsic mapping between a closed surface and the unit sphere.

Although we are still far from a completely satisfactory solution, we have made significant progress. Starting with the EGI, which can only handle convex objects under rotation, we have introduced the DEGI and the CEGI which can deal with translations and, to some extent, with non-convexity.

Finally, the SAI relaxes many of the constraints of the EGI-like representations by preserving the connectivity of the surface, that is, a connected path on the surface maps to a connected path on the sphere. This property allows us to deal with non-convex objects and with general transformations.

We are still a long way from a general solution, however. First of all, the SAI is limited to objects with a genus 0 topology. Second, the algorithm used for extracting the underlying deformable surface does have limitations with respect to the variation in the object shape.

Nevertheless, we believe that intrinsic coordinate maps are a fundamental tool for general object matching and we working toward improving the SAI to handle more general cases.

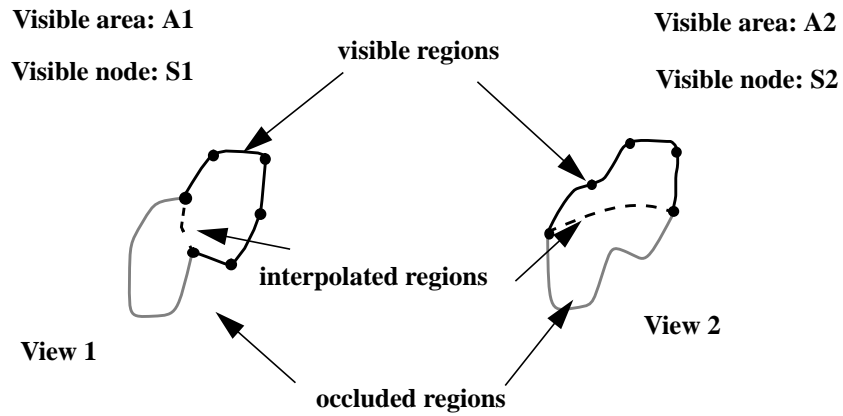


Figure 15: Matching partial views

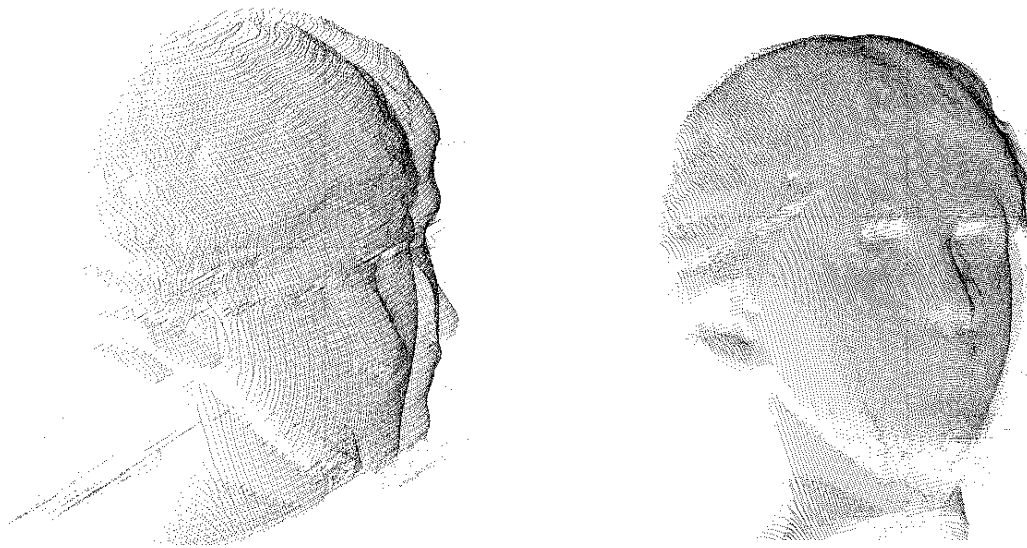


Figure 16: Merging two views; (a) Overlaid views before registration; (b) Overlaid views after registration.

visible areas of the object surface be A_1 and A_2 for V_1 and V_2 , respectively. The ratio of the number of visible SAI nodes to the total number of SAI nodes, S_o is equal to the ratio of the visible area to the entire object area, A_o

$$\frac{S_1}{S_o} = \frac{A_1}{A_o} \quad \frac{S_2}{S_o} = \frac{A_2}{A_o}:$$

However, we do not know A_o since we have only partial views of the object, but we can estimate A_1 and A_2 from each of the views. Eliminating S_o from these equations, we obtain $S_2 = S_1 \cdot A_2 / A_1$.

This equation enables us to modify the SAIs from different views so that the distribution of nodes in the visible area is consistent between views. More precisely, we compute the scale factor A_2/A_1 from the estimated visible areas from each of the images, and move the nodes of the SAI from V_2 so that the equation is satisfied.

The key in this procedure is the connectivity conservation property of the SAI. Specifically, if a connected patch of the surface is visible, then its corresponding image on the SAI is also a connected patch on the sphere. This property allows us to bring the two connected patches into correspondence using a simple spherical scaling. This property is the fundamental difference between the SAI and the spherical representations which cannot deal easily with partial views.

Figure 16 shows the final result of computing the transformation between the two views. Figure 16 (a) shows the superimposition of the data points from the two range images before computing the transformation. Figure 16(b) shows the same combined data set using the transformation computed using the algorithm above. This display shows that the two views are registered correctly.

corresponding to the node P of S , resp. P' . A first estimate of the transformation is computed by minimizing the sum of the squared distances between the points M of the first view and the corresponding points $R_o M' + T_o$ of the second view. The optimum transformation for E can be computed in a non-iterative manner by using standard quaternion-based techniques..

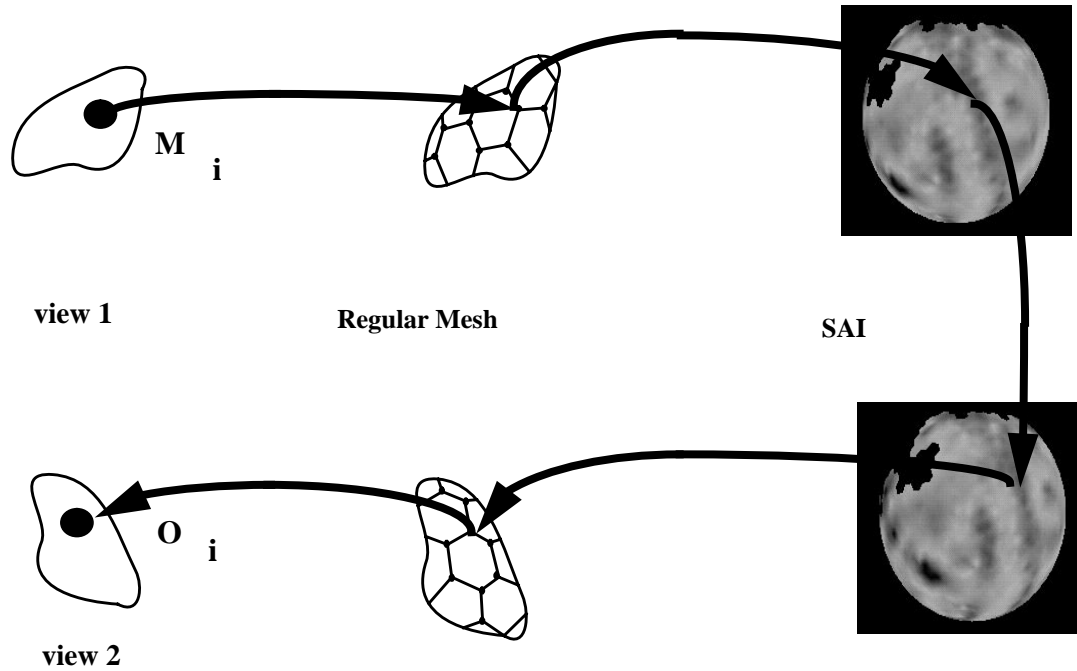


Figure 14: Computing the full transformation

3.8. Matching Surface Models

In order to compare SAIs computed from different views, we need to adjust the number of nodes because the relative sizes of the visible and hidden areas vary depending on the viewing direction. As mentioned before, the nodes which are in regions of the object where no data points were presented are explicitly marked as “interpolated”. As a result, the size of the visible and interpolated parts of the mesh can be easily identified.

Let us consider the problem of merging two views, V_1 and V_2 . Let S_1 and S_2 be the number of nodes that would be visible from V_1 and V_2 if we had a complete model of the object. Let the

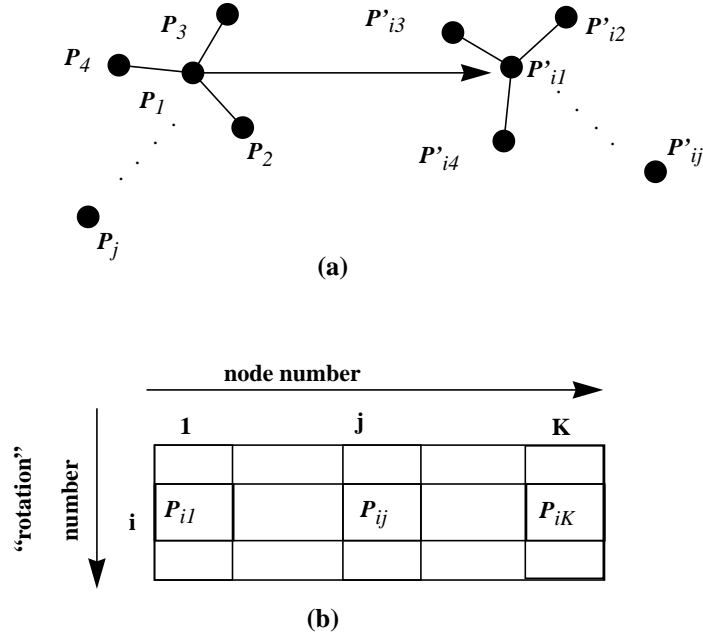


Figure 13: Efficient matching algorithm; (a) Valid correspondence

The row that produces the minimum D_i gives the best correspondence between nodes of the mesh, $\{(P_j, P'_{ij})\}$, which is used for computing the full transformation between the object meshes as described in the next section.

This algorithm is guaranteed to find the global optimum of D and it does not require an initial estimate of the transformation. It is efficient because all that is required at run time is to look up the correspondence table, to compute sum of square differences of corresponding nodes and to add them up

3.7. Computing the Full Transformation

The last step in matching objects is to derive the transformation between the actual objects, given the rotation between their SAIs (See Figure 14). The rotational part of the transformation is denoted by R_o , the translational part by T_o . Given a SAI rotation R , we know the corresponding node P' of each node P of S . Let M , resp. M' , be the point on the view

correspondences. Moreover, there is only a small number of such initial correspondences.

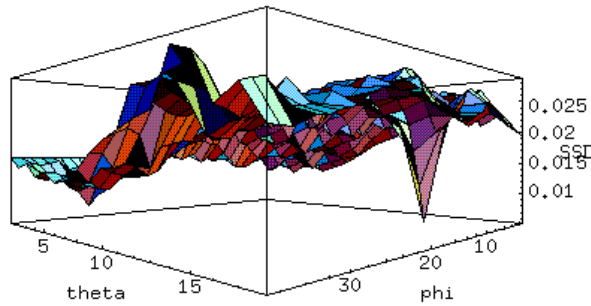
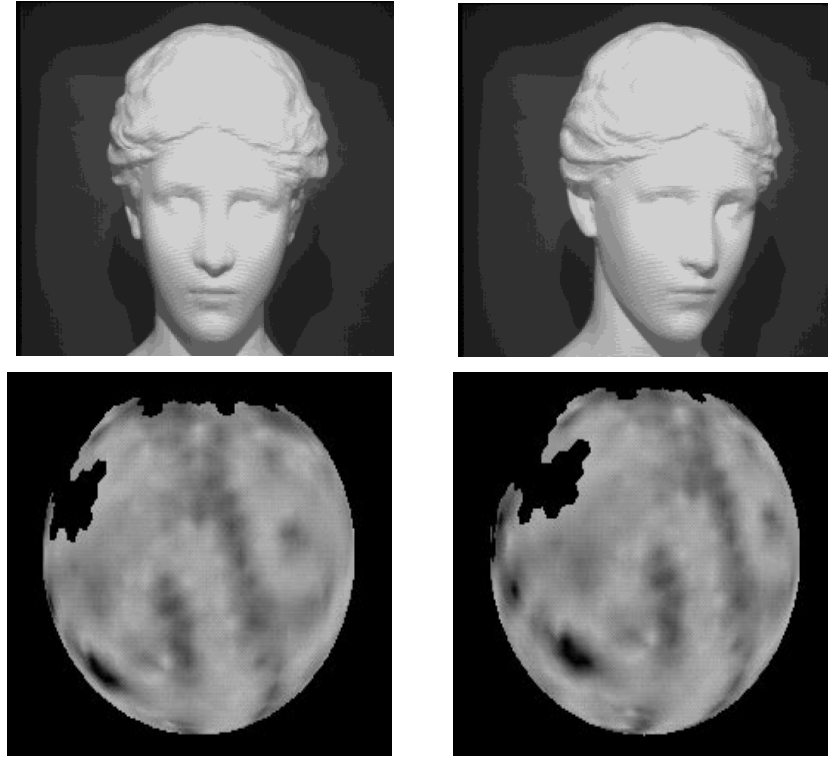


Figure 12: Matching two SAIs

Based on this observation, we developed an SAI matching algorithm decomposed into two stages: a pre-processing phase and a run-time phase. During pre-processing, we generate the data structure shown in Figure 13(b). The data structure is a two dimensional array in which each row corresponds to a possible rotation of the SAI and in which column j of row i is the index of the node P_{ij} corresponding to node P_j and correspondence number i . At run-time, the distance is evaluated for each row of the array: $D_i(S, S', R) = \sum (g(P_j) - g(P_{ij}))^2$

between the simplex angles at the nodes of one of the spheres and at the nodes of the rotated sphere. Formally, the distance is defined as: $D(S, S', R) = \sum (g(P) - g(RP))^2$

The minimum of D corresponds to the best rotation that brings S and S' in correspondence.

Figure 12 shows the result of matching two views of a head. Figure 12(a) shows the intensity images of the two views of the object. Figure 12(b) shows the corresponding SAIs. Figure 12(c) shows the distribution of D as a function of two of the rotation angles, ϕ and θ . The graph exhibits a sharp minimum corresponding to the best rotation between the two spherical maps.

The rotation of the SAIs is not the same as the rotation of the original objects; it is the rotation of the spherical representations. An additional step is needed to compute the actual transformation between objects as described below.

Figure 12 shows the graph of D as function of ϕ and θ obtained by sampling the space of all possible rotations, represented by three angles (θ, ϕ, ψ). Although convenient, this approach is too expensive to be practical.

An alternative matching algorithm is based on the observation that the only rotations for which $D(S, S', \mathbf{R})$ should be evaluated are the ones that correspond to a valid list of correspondences $\{(\mathbf{P}_i, \mathbf{P}'_j)\}$ between the nodes \mathbf{P}_i of S and the nodes \mathbf{P}'_j of S' . Figure 13(a) illustrates the correspondences between nodes: Node \mathbf{P}_1 of the first SAI is put in correspondence with node \mathbf{P}'_{i1} of S' and its two neighbors, \mathbf{P}_2 and \mathbf{P}_3 , are put in correspondence with two neighbors of \mathbf{P}'_{i1} , \mathbf{P}'_{i2} and \mathbf{P}'_{i3} , respectively. This set of three correspondences defines a unique rotation of the spherical image. It also defines a unique assignment for the other nodes, that is, there is a unique node \mathbf{P}'_{ij} corresponding to a node \mathbf{P}_i of S , given the initial

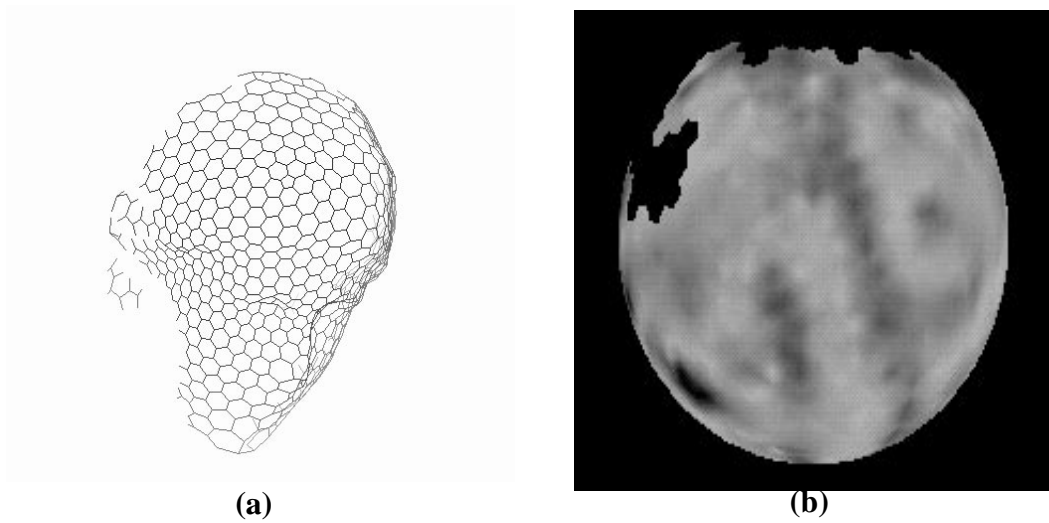


Figure 11: (a) Deformable mesh, (b) SAI representation on the unit sphere

3.6. Matching Surface Models

We now address the matching problem: Given two SAIs, determine the rotation between them, and then find the rigid transformation between the two original sets of points. The representations of a single object with respect to two different viewing directions are related by a rotation of the underlying sphere. Therefore, the most straightforward approach is to compute a distance measure between two SAIs. Once the rotation yielding minimum distance is determined, the full 3-D transformation can be determined.

In the following discussion, we will consider only the vertices of the SAIs that correspond to visible parts of the surface. Let S and S' be the SAIs of two views. S and S' are representations of the same area of the object if there exists a rotation \mathbf{R} such that $g(\mathbf{P}) = g(\mathbf{R}\mathbf{P})$ for every point \mathbf{P} of S .

The problem now is to find this rotation using the discrete representation of S and S' . This is done by defining a distance $D(S, S', \mathbf{R})$ between SAIs as the sum of squared differences

transformations.

3) A connected patch of the surface maps to a connected patch of the spherical image. It is this property that allows us to work with non-convex objects and to manipulate models of partial surface, neither of which are possible with conventional spherical representations.

Figure 10 (a) and (b) show an intensity image and the corresponding set of points from the range image. In this example, we use the dual of the 9th subdivision of a 20-face icosahedron, (1620 faces). This initial mesh is deformed and reaches the stable state shown in Figure 11(a). The corresponding SAI data is shown in Figure 11(b). In the SAI display, the distance from each vertex to the origin is proportional to the simplex angle.

In general, parts of the surface may be occluded by other parts of the object in the range image. The surface fitting algorithm interpolates smoothly across regions of occluded data. In addition, nodes of the mesh are flagged as interpolated or non-interpolated depending on their distances from the closest data point. Specifically, a node is marked as “interpolated” if the closest data point is at a distance greater than a threshold. The matching procedure then uses the interpolation flags to determine which nodes should be included in the matching function. The same mechanism is used in order to deal with backfacing regions of the surface. Additional issues on matching partial surfaces are discussed below.

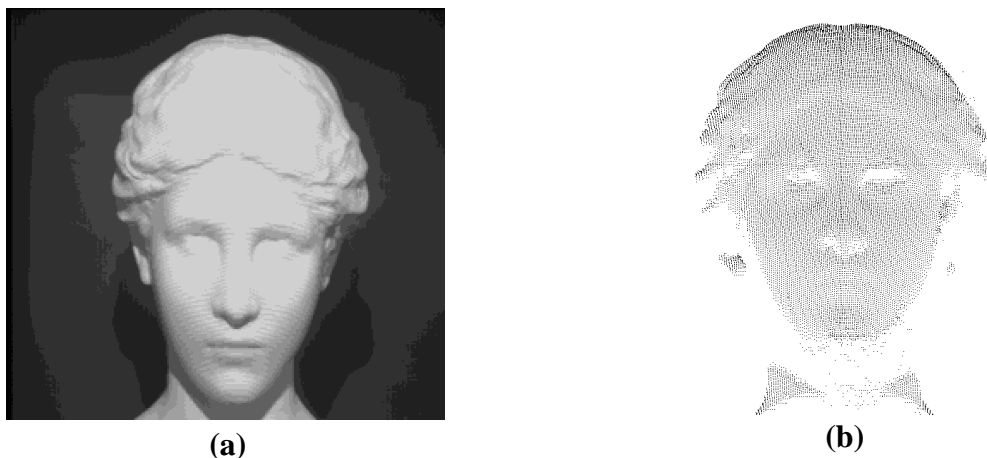


Figure 10: Input data: (a) Intensity image, (b) Range image

which is sufficient for matching purposes. Finally, $g(\mathbf{P})$ is invariant with respect to rotation, translation, and scaling.

3.5. Deformable Surface Mapping

A regular mesh drawn on a closed surface can be mapped to a spherical mesh in a natural way. For a given number of nodes K , we can associate with each node a unique index which depends only on the topology of the mesh and which is independent of the shape of the underlying surface. This numbering of the nodes defines a natural mapping h between any mesh M and a reference mesh S on the unit sphere with the same number of nodes: $h(\mathbf{P})$ is the node of S with the same index as \mathbf{P} .

Given h , we can store at each node \mathbf{P} of S the simplex angle of the corresponding node on the surface $g(h(\mathbf{P}))$. The resulting structure is a spherical image, that is, a tessellation on the unit sphere, each node being associated with the simplex angle of a point on the original surface. We call this representation the Spherical Attribute Image (SAI).

If the original mesh M satisfies the local regularity constraint, then the corresponding SAI has several invariance properties:

- 1) For a given number of nodes, the SAI is invariant by translation and scaling of the original object.
- 2) The SAI represents an object unambiguously up to a rotation. More precisely, if M and M' are two tessellations of the same object with the same number of nodes, then the corresponding SAIs S and S' are identical up to a rotation of the unit sphere. One consequence of this property is that two SAIs represent the same object if one is the rotated version of the other. It is this property which will allow us to match surfaces that differ by arbitrary rigid

good approximation of the object surface. We need to add another constraint in order to build meshes suitable for matching. Specifically, we need to make sure that the distribution of mesh nodes on the surface is invariant with respect to rotation, translation and scale.

Let us consider a 2-D case. If all the edges of the mesh have the same length, the tessellation is regular. Namely, the length PP_1 should be same as the length PP_2 . This condition is same as that P 's projection to the P_1P_2 , Q is at the center G .

We can extend this definition of the regularity to the 3D case. Let P be a node of the tessellation, P_1, P_2, P_3 be its three neighbors, G be the centroid of the three points, and Q be the projection of P on the plane defined by P_1, P_2 , and P_3 (See Figure 9). The local regularity condition simply states that Q coincides with G .

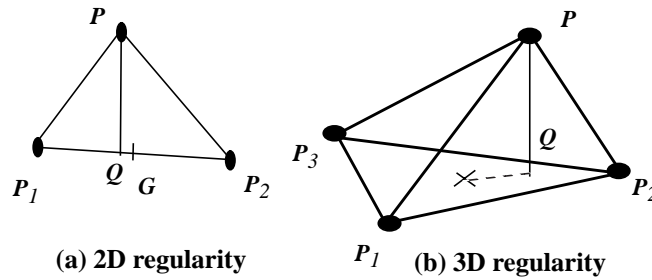


Figure 9: Regularity constraint

3.4. Discrete Curvature Measure

The next step in building a discrete surface representation is to define a measure of curvature that can be computed from a tessellation. Instead of estimating surface curvature by locally fitting a surface or by estimating first and second derivatives, we proposed a measure of curvature computed at every node from the relative positions of its three neighbors. We call this measure of curvature the simplex angle and we denote its value at node P by $g(P)$. Although $g(P)$ is not the curvature at P , it behaves as a qualitative measure of curvature

for many algorithms to have a constant number of neighbors at each node. We use a class of tessellations such that each node has exactly three neighbors. Such a tessellation can be constructed as the dual of a triangulation of the surface.

Let us first consider tessellations of the unit sphere. A regular tessellation would be a tessellation covering a complete spherical surface such that the distance between vertices is constant and each node has exactly three neighbors. It is well known that only approximate global regularity can be achieved. Specifically, the approach that we use is to first build a triangulation by subdividing each triangular face of a 20-face icosahedron into N smaller triangles. The final tessellation is built by taking the dual of the N^2 faces triangulation, yielding a tessellation with the same number of nodes. This tessellation of a sphere, a geodesic dome, is the starting point of our technique. Figure 8 shows an example of a 1620-face semi-regular geodesic dome.

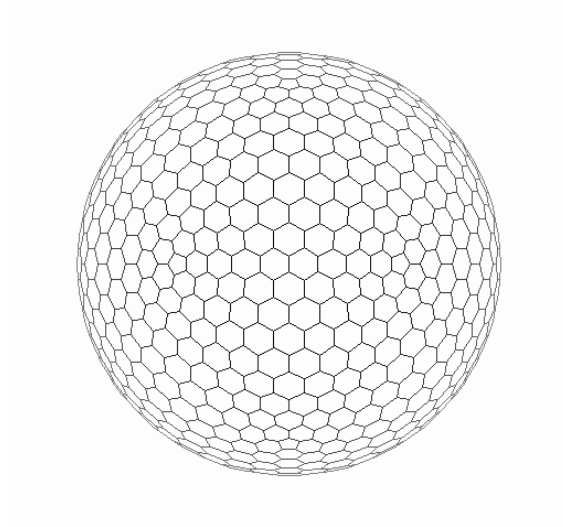


Figure 8: Semi-regular geodesic dome

3.3. Regularity Constraint

In order to obtain a mesh of an arbitrary surface, we deform a tessellated surface until it is a

invariants, Gaussian curvature is the most important. The distribution based on the Gaussian curvature is referred to as the Spherical Attribute Image (SAI).

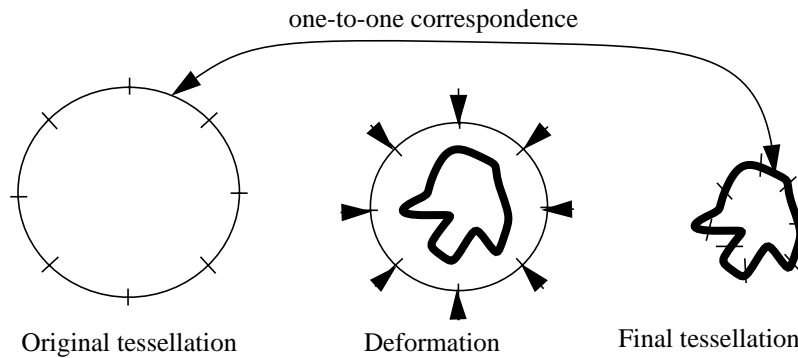


Figure 7: Deformable surface mapping

At each tessellation on the object surface, we calculate invariants such as Gaussian curvature or surface albedo, and map them to the corresponding original tessellation of the geodesic dome. We can observe a distribution of invariants on the unit sphere. Among the possible invariants, Gaussian curvature is the most important. The distribution based on the Gaussian curvature is referred to as the Spherical Attribute Image (SAI).

In the following section, we will briefly describe the SAI. First, we explain how to tessellate an arbitrary surface into a semi-regular mesh, and how to calculate the simplex angle (discretized Gaussian curvature), a variation of curvature, at the nodes of the mesh, and how to map the mesh to a spherical image. Finally, we discuss how to handle partial views of 3-D objects.

3.2. Semi-Regular Tessellation

A natural discrete representation of a surface is a graph of points, or tessellation, such that each node is connected to each of its closest neighbor by an arc of the graph. It is desirable

3. Spherical Attribute Image

3.1. A Novel Mapping Based On Deformable Surface

The fundamental problem of the EGI family is that it depends on the Gauss mapping. For that reason, more than two parts on an object surface may be mapped on the same point of the sphere. More than two objects may have the same EGI. Further, a partial EGI from a part of an object is not same as a part of EGI from the whole object. Thus, under occlusion, we cannot perform the EGI matching. This problem is due to the fact that the Gauss mapping is not unique for non-convex objects.

We have derived a novel method to make a one-to-one mapping between a non-convex object surface and a spherical surface [11,13]. The method uses a deformable surface. We first prepare a semi-regularly tessellated geodesic dome (a tessellated unit sphere). Then, we deform the geodesic dome onto an object surface as close as possible (data force) while maintaining the local regularity constraint (regularization force): to ensure that tessellations have a similar area and the same topology as one another. The final representation is given as the equilibrium between the data force and the regularization force. By doing so, 1) the object surface is semi-uniformly tessellated, 2) each tessellation on the object surface has a counterpart on the undeformed geodesic dome (unit sphere); thus, we can establish a one-to-one mapping between the object surface and the unit sphere. The mapping is referred to as deformable surface mapping (DSP) (see Figure 7).

At each tessellation on the object surface, we calculate invariants such as Gaussian curvature or surface albedo, and map them to the corresponding original tessellation of the geodesic dome. We can observe a distribution of invariants on the unit sphere. Among the possible

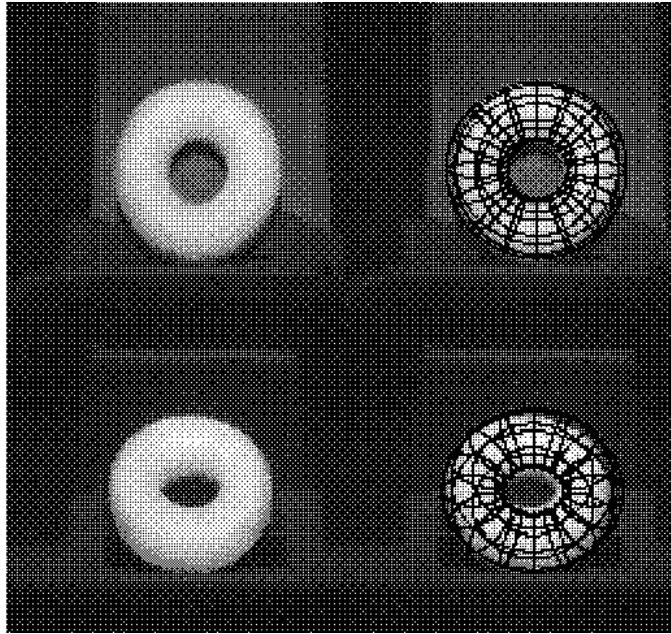


Figure 6: Localization results using CEGI.

tion is the signed distance of the oriented tangent plane from a predefined origin. He proposes to ascribe to each different surface a separate support function value. This means that, in general, the proposed variant of the Gauss map of a surface is not globally one to one. Although it is less compact it can uniquely determine a surface. A method to determine object pose based on this representation was not presented in Nalwa's paper.

Roach et al. [10] encode positional information by expressing the equation of a surface patch in dual space. The resulting encoded representation is called the spherical dual image. A point in the dual space represents both the orientation and position of a patch; edges are explicitly described as connections between dual points. A drawback of this approach is that planes passing near or through the designated origin cannot be dualized properly; they map to infinity or very large values.

Hence, for each point of the CEGI, the magnitude of the weight is independent of the translation. The complex number wraps around for every translation distance of 2π . Therefore, the computed translation is known only up to 2π . To eliminate this ambiguity, all distances are normalized such that the greatest expected change in translation distance is π .

2.3.2. Pose Determination Strategy

Given a prototype CEGI and a partial CEGI of an unknown object, we can recognize the object and determine its orientation as follows: First, we calculate the magnitude distributions of both CEGI's, and second, we match the resulting distribution with that of the prototype. Once both the object and its orientation with respect to the stored model are identified, the object translation can be calculated by using the suitably oriented CEGI's.

The translation parameters can be determined by applying a least-squares techniques as follows: Suppose that the object has been translated by δx , δy , and δz in the x , y , and z , respectively. Then, the weight Ae^{jd} of a surface patch becomes $Ae^{j(d + \delta\vec{d} \cdot \vec{n})}$ after translation, where $\delta\vec{d} = \delta x\vec{i} + \delta y\vec{j} + \delta z\vec{k}$ and $\vec{n} = n_x\vec{i} + n_y\vec{j} + n_z\vec{k}$. Then, for each matched weight $P_{\vec{n}_i}$ in the object CEGI corresponding to the weight $P_{\vec{n}_i}$ in the model CEGI, let

$$\begin{aligned} \omega_i &= \arg\left(\frac{P_{\vec{n}_i}}{P_{\vec{n}_i}}\right) = \arg\left(\frac{A_{\vec{n}_i} e^{j(d_i + \delta\vec{d} \cdot \vec{n}_i)}}{A_{\vec{n}_i} e^{jd_i}}\right) \\ &= \delta x n_{ix} + \delta y n_{iy} + \delta z n_{iz} \end{aligned}$$

The translation is computed by minimizing:

$$\varepsilon = \sum_{i=1}^{N_{visible}} (\omega_i - n_{ix}\delta x - n_{iy}\delta y - n_{iz}\delta z)^2$$

where $N_{visible}$ is the total number of visible surface patches on the object.

Figure 6 shows the localization results of a non-convex curved object using CEGI.

Similar representations have been proposed by Nalwa [9]. He proposed that a surfaces be represented by their Gaussian images augmented by the support function. This support func-

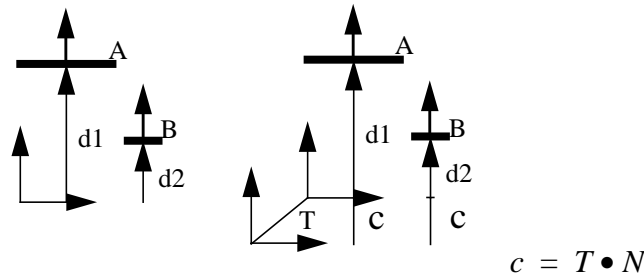
For any given point in the CEGI corresponding to normal \hat{n} , the magnitude of the point's weight is Ae^{jd} . A is independent of the normal distance, and if the object is convex, the distribution of A corresponds to the conventional EGI representation. If the object is not convex, the magnitude of each weight will not necessarily be equal to the weight in the corresponding conventional EGI.

The translation invariant property of the weight magnitude applies even if there is more than one contiguous surface patches with the same normal. Consider the surface patches whose normal are \hat{n} shown in Figure 5 (the distribution d_1, \dots, d_k is henceforth referred to as the surface normal distance distribution).

Before translation, the corresponding complex weight is $P = \sum_{i=1}^k A_i e^{jd_i}$

After a translation along a vector T , the complex weight becomes:

$$P' = \sum_{i=1}^k A_i e^{j(d_i + T \cdot \hat{n})} = e^{j(T \cdot \hat{n})} P$$



$$\begin{aligned}
 P &= Ae^{jd1} + Be^{jd2} \\
 P' &= Ae^{(jd1 + jc)} + Be^{(jd2 + jc)} \\
 &= \left(Ae^{jd1} + Be^{jd2} \right) e^{jc} = P e^{jc}
 \end{aligned}$$

Figure 5: Translation effect on CEGI

2.3. Complex EGI

2.3.1. Definition

One of the problems with the EGI is that we can determine the rotation of an object but cannot determine the translation of the object. In order to recover translation, we have introduced the complex EGI to encode positional information.

We will assume some arbitrary origin of an object. We will measure the distance, d , from this origin to each surface patch. We will store d at the corresponding point of the Gaussian sphere. The CEGI weight at each point on the Gaussian sphere is a complex number whose magnitude is the surface area and whose phase is the distance information. When an object translates, the magnitude of the complex mass remains the same while its phase changes accordingly.

Object recognition is accomplished by EGI matching using the magnitude only. The translation component is computed by using the phase difference.

Formally, the complex weight associated with a surface patch is Ae^{jd} , where A is the area of a patch with surface normal \vec{n} , the normal distance d to a fixed origin (Figure 4). The distance d is positive if the perpendicular vector from the origin to the patches is in the same direction as the outward facing normal of the patch.

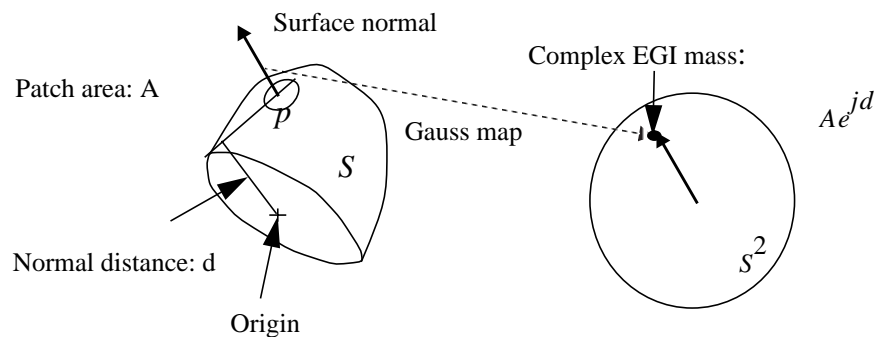


Figure 4: Complex EGI (CEGI)

point on the Gaussian sphere. However, when an object is observed from a particular viewing direction, some of the area (such as region A) is occluded when viewed from this direction and does not contribute EGI mass on the Gaussian sphere. Thus, the observed EGI is not same as the corresponding part of the model EGI on the Gaussian sphere.

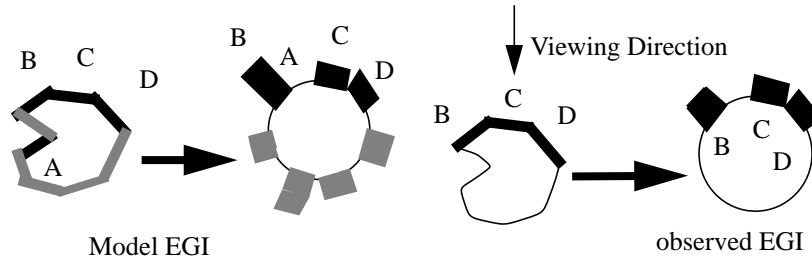


Figure 2: EGI of a non-convex object

In order to avoid this effect, we have derived a distributed EGI [7]. This method recalculates a partial EGI for each viewing direction.

We can represent all possible viewing directions using a viewing sphere. Thus, we sample a viewing sphere into sampling viewing directions. At each sampling viewing direction, we recalculate EGI by considering the effect of self occlusion. Since this effect is accommodated in the model, we can determine the attitude of a non-convex object using this distributed EGI.

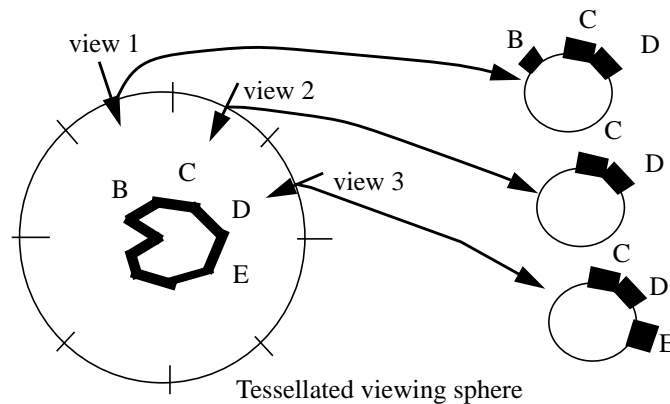


Figure 3: Definition of Distributed EGI

over the Gaussian sphere. This mass distribution depends on the shape of the object and is referred to as the Extended Gaussian Image (EGI) of the object.

This mapping does not incorporate the original spatial relationship between surface patches. Thus, it seems that the original shape information is somehow reduced. However, Minkowski proved that, if two convex objects have the same EGIs, those objects are congruent [2]. Other important characteristics of EGI are [3]:

- The EGI mass on the sphere is the inverse of Gaussian curvature on the object surface,
- The mass center of the EGI is at the origin of the sphere,
- As an object rotates, its EGI also rotates in the exact same way.

Using the Minkowski theorem, we can develop an object recognition system. From an object model, we sample its surface evenly, calculate surface normal, and obtain the model EGI. After obtaining the surface normal distribution of an observed object, we can repeat the same process to build an observed EGI. By examining which model EGI has a distribution similar to the observed one, we can recognize the observed object; by examining which part of the EGI distribution corresponds to the observed partial EGI, we can determine from which direction we are observing it. Some of the earlier work on object recognition using EGI are found in [4, 5, 6].

2.2. Distributed EGI

The utility of the original EGI is strictly limited to convex objects. A non-convex object has more than two separated regions with the same surface orientations. Such areas, though physically separated (for example, regions A and B in Figure 2), will be mapped to the same

2. Gauss Mapping and Related Representations

Gauss derived a mapping method that uses surface orientations to map points on an arbitrary curved surface onto points on the sphere [1]. Let us assume a surface patch p on a curved surface. At that surface patch, we can define the surface normal $N(p)$ uniquely (Figure 1). Regardless of the position of p , we can translate the normal vector so that its origin coincides with the origin of the coordinate system. The end point of the unit normal lies on a unit sphere. The mapping that associates this point on the unit sphere with the patch is referred to as a Gauss map and the sphere is referred to as a Gaussian sphere.

Formally, let $S \subset R^3$ be a surface with an orientation N . The map $N: S \rightarrow R^3$ takes its values in the unit sphere S^2

The map $N: S \rightarrow S^2$, thus, defined, is called the Gauss map of S (See Figure 1.)

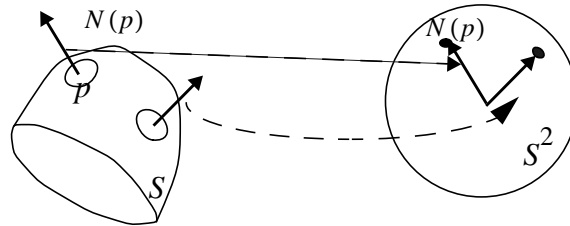


Figure 1: The Gauss Map

2.1. Extended Gaussian Image (EGI)

Let us assume that an object surface is evenly sampled into patches. At each surface patch, we can define a surface normal with a single unit of mass. Each surface normal is assumed to be able to vote the mass to the corresponding point on the Gaussian sphere. From the voting by the all surface patches over the object surface, we can observe a distribution of mass

surface do carry useful information, such as curvature, for recognition.

It is desirable to assign a coordinate system to curved surfaces and to use invariant features, including curvature distributions, along this particular coordinate system. This coordinate system should be independent of the viewing direction. Since it is difficult to reliably segment a curved surface into regions, it is also desirable to define a coordinate system over the entire object surface.

Aspherical representation maps an entire object surface to a standard coordinate system (a unit sphere). Objects usually handled by vision systems have closed surfaces: topologically equivalent to a spherical surface. Thus, we began our effort to develop a mapping method from an arbitrary object surface to a spherical surface and store invariants over the spherical surface. It is possible to define a coordinate system on a surface using two parameters such as longitude and latitude. Such parametrization, however, require specific information, that is, the direction of an imaginary line between North and South poles.

This paper briefly overviews our earlier efforts on such spherical representations. We begin with a discussion of the Extended Gaussian Image developed around 1980, and, continue on to describe our recent work on the Spherical Attribute Image.

1. Introduction

One of the fundamental problems in object recognition is how to represent the objects models. The representation govern the characteristics and efficiencies of recognition systems. We restrict ourselves here to surface-based representations since those are the most relevant in computer vision.

A surface-based representation describes an object as a collection of visible “faces” of the object. Since imaging systems provide the same information as surface-based representations, it is relatively easy to use surface-based representation for object recognition. Representative surface-based representations include edge-and/or face-based invariants, aspect graphs, and spherical representations.

The simplest type of object representation is based on planar faces. A planar face has a clear boundary of surface orientation discontinuity and its internal pixels provide less information. A polyhedron, consisting of planar faces, effectively represents the relations between faces for recognition. Early works by Oshima-Shirai [14] and Bolles [15] effectively use such graphs of visible face relations.

One of the basic problems in using such visible graphs was determining the number of different graphs required to represent one object. Koendering’s aspect answers this question [16]. The aspect representation specifies an object as a collection of all possible topologically different relational graphs of visible faces. Our earlier work on the vision algorithm compiler used this aspect representation for object recognition.

For curved object recognition, the boundary of a curved surface patch is often ill-defined; the relative relationships between faces are unreliable. Fortunately, however, points on the

Abstract

One of the fundamental problems in representing a curved surface is how to define an intrinsic, i.e., viewer independent, coordinate system over a curved object surface. In order to establish point matching between model and observed feature distributions over the standard coordinate system, we need to set up a coordinate system that maps a point on a curved surface to a point on a standard coordinate system. This mapping should be independent of the viewing direction. Since the boundary of a 3-D object forms a closed surface, a coordinate system defined on the sphere is preferred.

We have been exploring several intrinsic mappings from an object surface to a spherical surface. We have investigated several representations including: the EGI (Extended Gaussian Image), the DEGI (Distributed Extended Gaussian Image), the CEGI (Complex Extended Gaussian Image), and the SAI (Spherical Attribute Image). This paper summarizes our motivations to derive each representation and the lessons that we have learned through this endeavor.

Keywords: Computer Vision, Scene Understanding, Robotics, Object Representation, Gauss Map, Gaussian Sphere, Differential Geometry

Spherical Representations: from EGI to SAI

Katsushi Ikeuchi and Martial Hebert

October 1995
CMU-CS-95-197

School of Computer Science
Carnegie Mellon University
Pittsburgh, Pennsylvania 15213-3890

The research is sponsored in part by the Advanced Research Projects Agency under the Army Research Office under Grant DAAH04-94-G-0006, and in part by National Science Foundation under Grant IRI-9224521.

The views and conclusions contained in this document are those of the authors, and should not be interpreted as representing the official policies, either expressed or implied, of NSF, ARPA, or the U.S. government.